2017 IEEE International Conference on Telecommunications and Photonics (ICTP)
26-28 December, 2017, Dhaka, Bangladesh

Effect of Core Infiltration in the Birefringence of Photonic Crystal Fiber

Saleha Fatema†, Rubaya Absar†, Mohammad Istiaque Reja, and Aobaida Akhtar*

Department of Electrical and Electrical Engineering, Chittagong University of Engineering and Technology Chittagong-4349, Bangladesh

† Two first author made equal contribution

*lilyjobaida@cuet.ac.bd

***Abstract*—The effect of core infiltration in the birefringence of Photonic Crystal Fiber (PCF) is investigated. An elliptical soft glass rod infiltration is introduced in the core region of the fiber as it provides greater refractive index contrast between the core and the cladding. This modification also creates asymmetry in the core of the fiber which results in a resilient birefringence. Four structures (Hexagonal, Octagonal, Decagonal and Elliptical) are investigated and a comparative study is made to observe the change in birefringence due to the infiltration. It is observed that, by introducing this infiltration the birefringence is improved up to the order of 10^{-1}. The birefringence is increased 4.82×10^6 times in the hexagonal PCF, 5.38×10^5 times in octagonal PCF, 546 times in decagonal PCF and about 8 times in the elliptical PCF at operating wavelength due to the core infiltration. The numerical investigation of the structure is conducted using full vector finite element method. The fabrication imperfection possibility is considered by analyzing $\pm 2\%$ tolerance in fiber dimension.**

***Index Terms*—Photonic crystal fiber; Core infiltration; Birefringence; Refractive index contrast; Full vector finite element method;**

I. Introduction

Photonic Crystal Fiber, aims to address the challenge of higher channel capacity with increased data rate [1], has developed into being a well established area of research and commercialization. The main reason behind its growth is its ability to provide extra degrees of freedom in manipulating the optical properties of fiber such as high birefringence [2], ultra flattened dispersion [3], high nonlinearity [4], low confinement loss [5], endlessly single mode [6]. This is achieved by adjusting its structural parameters like pitch (Λ), air hole diameter (d) and shape, air filling ratio (d/Λ). This control over the optical properties of the fiber allows it to use in a wide range of application [7] instead of being limited to optical communication. One of the major fields of application is its uses as polarization maintaining fiber.

Polarization maintaining (PM) fibers play a very important role in high bit-rate optical transmission [8], fiber optic sensing [9], interferometry [10] and quantum key distribution systems [11]. It is also used in telecommunications for the connection between a source laser and a modulator [12]. Recently, PANDA (Polarization Maintaining and Absorption Reducing Fibers) [13], bow-tie [14] and elliptical jacket fibers [15] are used for polarization maintaining applications. These fibers operate by applying stress in the core region. Their modal birefringence is due to stress in the core region is up to 5×10^{-4} [16]. These stresses impose unpredictable and uncontrolled birefringence on the fiber [17]. On the other hand, a controllable birefringence can be obtained by using polarization maintaining photonic crystal fibers [18].

To improve this highly growing technology, researchers are now introducing newer concepts in the design of photonic crystal fibers like creating various defects in the core or cladding , use of liquid or gaseous materials and materials with greater refractive index or lower refractive index than silica in the core or cladding respectively. In this article, we have modified the typical photonic crystal fibers with an elliptical soft glass rod in the core region. The material of this elliptical glad rod is selected as SF57 as it has greater refractive index than silica which provides a greater index contrast between the core and the cladding resulting in asymmetry in the core and cladding and thus the birefringence is increased significantly.

II. Design and theory

An elliptical soft glass (SF57) rod is proposed in the core of four typical structures of PCF with circular air holes in the cladding. The cladding assembles multiple air hole rings. The background material is fused silica. For hexagonal structured PCF, the air hole diameters of 1^{st}, 2^{nd}, 3^{rd}, 4^{th}, 5^{th} rings are given as, d_1=d_2=d_3=d_4=d_5=0.5 μm where, d_1, d_2, d_3, d_4, d_5 are the diameter of 1^{st}, 2^{nd}, 3^{rd}, 4^{th}, 5^{th} ring respectively. The pitch, Λ of the structure is 1 μm and the air filling ratio, d/Λ is 0.5. The major and minor axis of the elliptical glass rod is 0.8 μm and 0.2 μm respectively. For octagonal structured PCF, the air hole diameters of 1^{st}, 2^{nd}, 3^{rd}, 4^{th}, 5^{th} rings are given as, d_1=d_2=d_3=d_4=d_5=0.665 μm. The pitch, Λ of the structure is 0.95 μm and the air filling ratio, d/Λ is 0.7. The major and minor axis of the elliptical glass rod is 0.6 μm and 0.2 μm respectively. For decagonal structured PCF, the air hole diameters of 1^{st}, 2^{nd}, 3^{rd}, 4^{th}, 5^{th} rings are given as, d_1=d_2=d_3=d_4=d_5=0.5 μm. The pitch, Λ of the structure is 1 μm and the air filling ratio, d/Λ is 0.5. The major and minor axis of the elliptical glass rod is 0.9 μm and 0.2 μm respectively. For elliptical PCF, the air hole diameters of 1^{st}, 2^{nd}, 3^{rd}, 4^{th}, 5^{th}, 6^{th} rings are given as, d_1=0.28 μm, d_2=0.30 μm, d_3=0.32 μm, d_4=0.34 μm, d_6=0.36 μm, d_6=0.4 μm. The major axis of the glass rod is 0.8 μm and minor axis is 0.2 μm. In all four cases the central elliptical portion of the core is filled with SF57 glass rod. Since SF57 has higher refractive index than silica, this modification improvises the performance of the fiber by creating asymmetry which leads to an ultra high birefringence. It also enhances the overall field confinement. Fig. 1 represents the cross sectional view of the investigated structures.

The full vector finite element method with perfectly matched layer is used to solve Maxwell's equation. The refractive index

978-1-5386-3374-8/17/$31.00 ©2017 IEEE

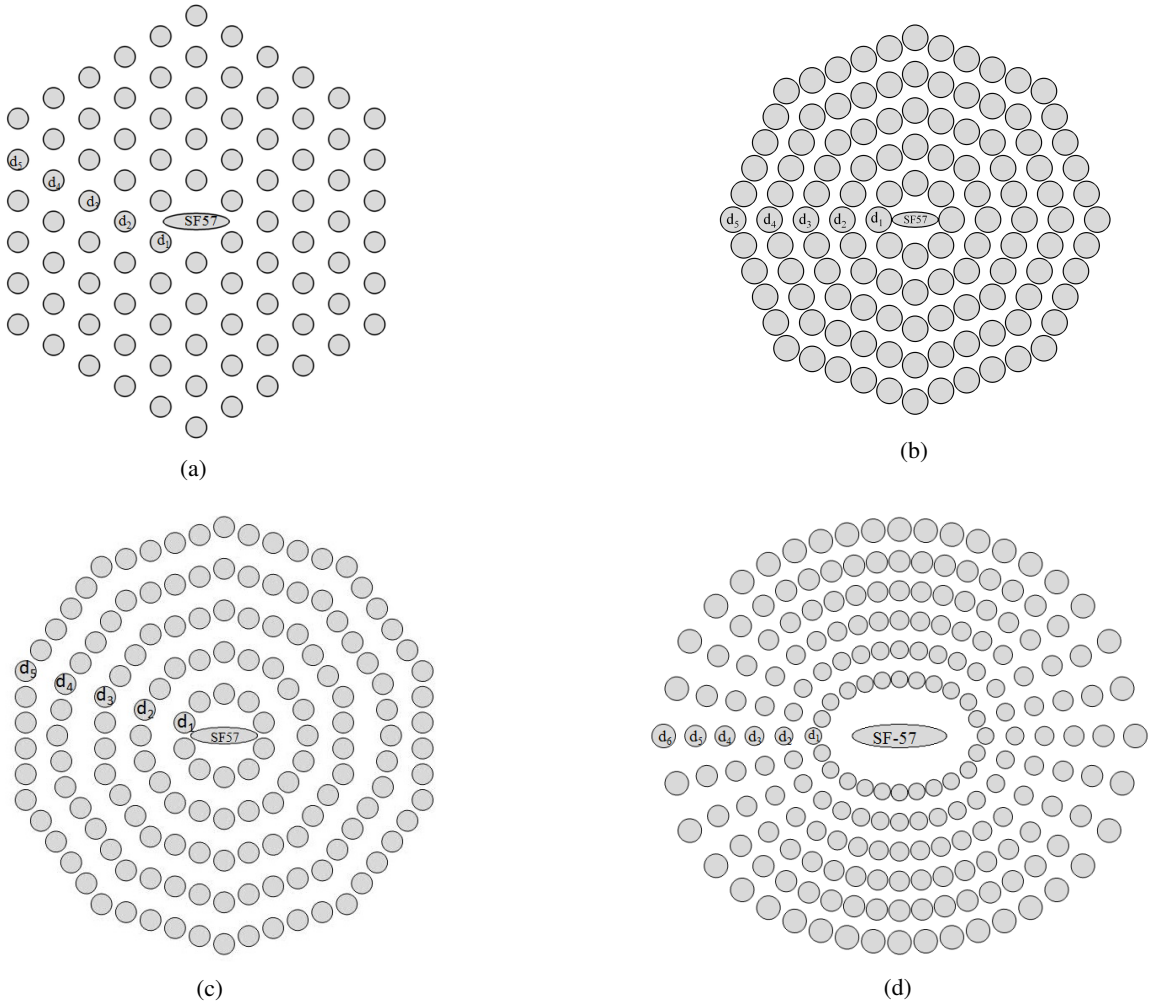

(a) (b) (c) (d)

Fig. 1: Cross sectional view of (a) hexagonal PCF (b) octagonal PCF, (c) decagonal PCF, (d) elliptical PCF with proposed infiltration where, d_1, d_2, d_3, d_4, d_5, d_6 are air hole diameters.

of the material is investigated over wavelength range from 1.3 μm to 1.7 μm covering E, S, C, L, U bands. The wavelength dependent refractive index of background material silica [19] and infiltration SF57 found by Sellmeier equation is included in simulation. The equation is given in (1)

$$n^2(\lambda) = 1 + \sum_i \frac{B_i \lambda^2}{(\lambda^2 - C_i)} \tag{1}$$

Here, n = refractive index; λ = wavelength; B_i (i=1,2,3) and C_i (i=1,2,3) are Sellmeier coefficients for specific material. Solving the eigenvalue problem by simulation, effective refractive index n_{eff} and effective area A_{eff} are obtained. Birefringence is obtained from the difference between effective refractive index of both x and y mode using (2)

$$B = |n_{effx} - n_{effy}| \tag{2}$$

Here, n_{effx} and n_{effy} are the effective refractive index for x-mode and y-mode respectively.

The single modeness of the fiber is verified by using V_{eff} parameter. The parameter is calculated by (3)

$$V_{eff} = \frac{(k \times \Lambda \times \sqrt{(A.F)})}{\lambda} \times \sqrt{(n_{eff}^2 - n_{air}^2)} \tag{3}$$

Where, K=$\frac{2\pi}{\lambda}$; λ=Wavelength; Λ=pitch; A.F=Air filling ratio; n_{eff}=Real part of effective refractive index; n_{air}= Refractive index of air.

It is known that, the fiber is considered as single mode if the value of V_{eff} is lesser than 2.40 [20]. In this paper, the proposed four structures satisfy this condition so they are considered as single mode fiber. The calculated value of V_{eff} over the wavelength 1.3 μm to 1.7 μm is plotted in the Fig. 2

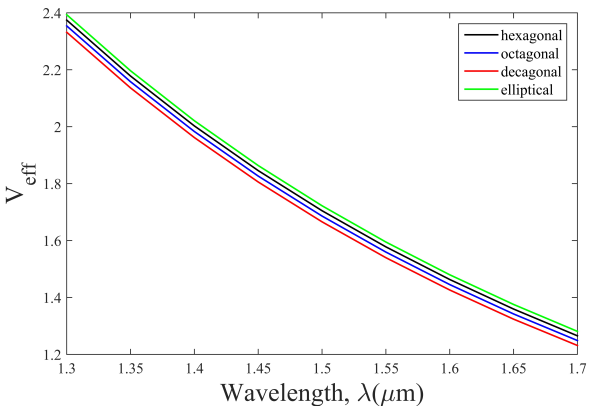

Fig. 2: V-parameter versus wavelength of the proposed structures with infiltration.

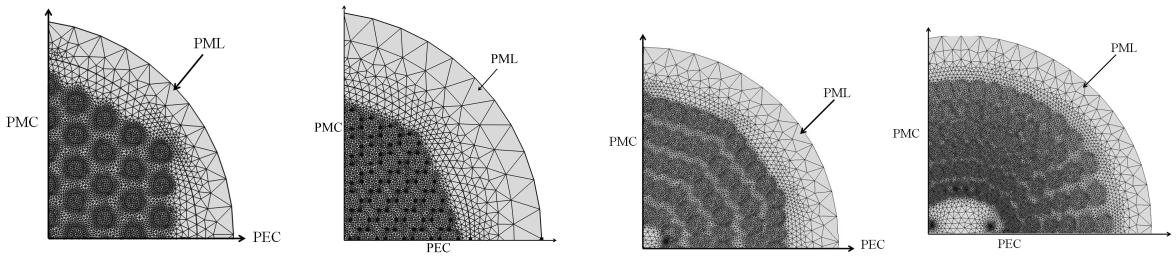

(a) (b) (c) (d)

Fig. 3: FEM mesh and boundary condition of (a) hexagonal infiltrated core PCF, (b) octagonal infiltrated core PCF, (c) decagonal infiltrated core PCF, (d) elliptical infiltrated core PCF.

III. Results and Discussion

The simulation is performed using COMSOL Multiphysics. The fibers are divided into 53570 triangular elements with 401505 degree of freedom. Fig. 3 shows the corresponding mesh formation of the simulation.

Investigations were performed on some structures of PCF. Analysis shows that these structures exerts poor optical properties and are not suitable for any practical application. It is found that, if an elliptical soft glass rod of higher refractive index than silica is inserted in the core region of the fiber, due to increase of index contrast, light is propagated in a more confined way through the core. Besides it also introduces an asymmetry which leads to a higher birefringence. This enhances the polarization maintenance capability of the fiber so the fiber can be used in various polarization maintaining applications. The effect of this core infiltration on birefringence of different structures of photonic crystal fiber has been discussed here.

Electric and magnetic fields are distributed in the x-y plane and the wave propagates in the z direction. Electric field vector distribution of the two fundamental modes is transversely related. The difference of effective refractive index between two fundamental modes is defined as birefingence.

Fig. 4, Fig. 5, Fig. 6, Fig. 7 show the change of birefringence with wavelength of the investigated structures and the modified structures. It can be shown from the figures that birefringence increases gradually when the wavelength increases from 1.3 μm to 1.7 μm as the modal effective area increases with increasing wavelength. By investigating Fig. 4a, Fig. 5a, Fig. 6a, Fig. 7a it can be observed that the structures without the infiltration exert very low value of birefringence.

On the other hand, when infiltration is added, the value of birefringence is increased considerably since electric field distribution is dominated highly due to addition of the slot effect as shown in the Fig. 4b, Fig. 5b, Fig. 6b, Fig. 7b.

Birefringence of the hexagonal structured PCF with and without infiltration is shown in Fig. 4. At operating wavelength, 1.55 μm, birefringence of the structure without infiltration is found to be 5.517×10^{-8} and that of with infiltration is 2.67×10^{-1} which is about 4.82×10^{-6} times greater than before. Birefringence of the octagonal structured PCF with and without infiltration is shown in Fig. 5. At operating wavelength, 1.55 μm, birefringence of the structure without infiltration is found to be 7.779×10^{-8} and that of with infiltration is 4.0185×10^{-2} which is about 537987 times greater than before. Birefringence of the decagonal structured PCF

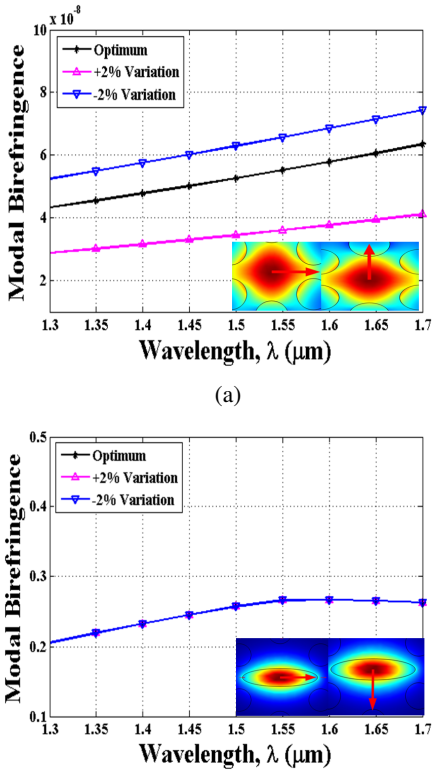

(a)

(b)

Fig. 4: Wavelength response of birefringence with $\pm2\%$ variation of hexagonal PCF (a) without infiltration, (b) with infiltration.

with and without infiltration is shown in Fig. 6. At operating wavelength birefringence of the fiber without infiltration is found to be 9.16×10^{-5} and that of with infiltration is 5×10^{-2} which is about 546 times greater than before. Birefringence of the elliptical PCF with and without infiltration is shown in Fig. 7. At operating wavelength the value of birefringence without infiltration is reported 6.828×10^{-3} and that of with infiltration is 5.244×10^{-2} which is about 8 times greater than before. It can be observed from these figures that the introduction of infiltration in the core region highly improve the birefringence. Since $\pm1\%$ variation may occur while fabrication [21], $\pm2\%$ tolerance has been taken under consideration for the fibers.

Table I summarizes the birefringence of the four investigated structures before and after adding the proposed modification. The comparison table clearly shows that the insertion of elliptical glass rod of the material SF-57 in the core region

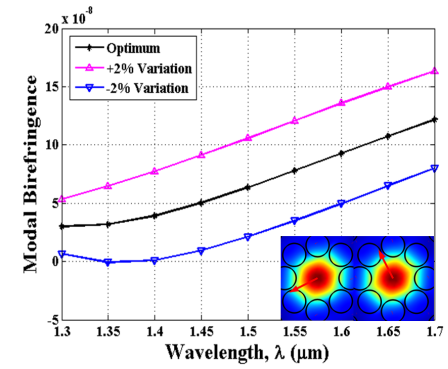

(a)

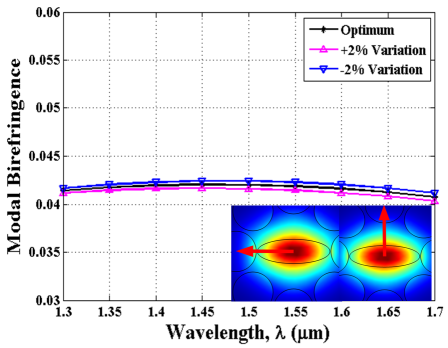

(b)

Fig. 5: Wavelength response of birefringence with $\pm 2\%$ variation of octagonal PCF (a) without infiltration, (b) with infiltration.

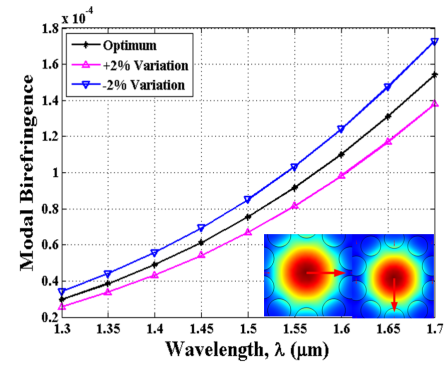

(a)

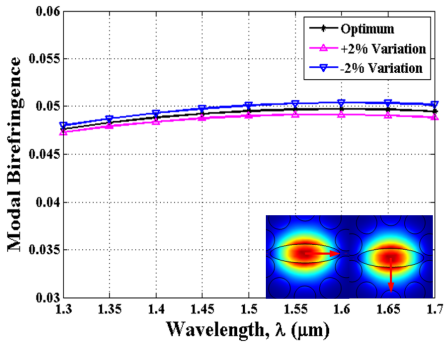

(b)

Fig. 6: Wavelength response of birefringence with $\pm 2\%$ variation of decagonal PCF (a) without infiltration, (b) with infiltration.

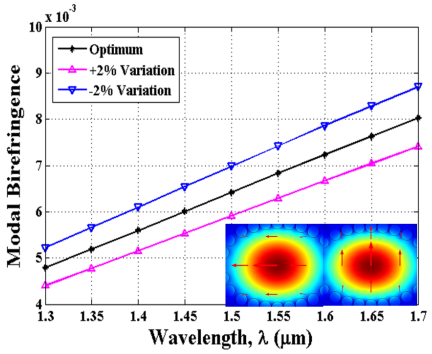

(a)

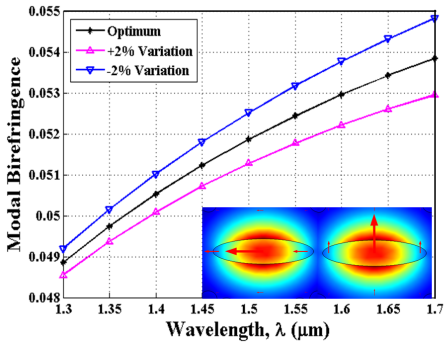

(b)

Fig. 7: Wavelength response of birefringence with $\pm 2\%$ variation of elliptical PCF (a) without infiltration, (b) with infiltration.

increases all the birefringence significantly.

Fabrication is a challenging issue when we are designing a PCF. PCF is fabricated using stack and draw process. Preform is made by stacking silica capillaries and a silica rod into a silica jacketing tube [22]. The preform is then drawn into fiber. Recently, significant development of the fabrication process permits fabrication of various complex structures [23] with reduced air hole diameter up to 110 nm [24]. Since smallest

TABLE I: Comparison of birefringence of different photonic crystal fiber without and with infiltration

Structure	Birefringence		
	Without Infiltration	With Infiltration	Increment factor
hexagonal	5.517×10^{-8}	2.67×10^{-1}	4.82×10^{6}
Octagonal	7.779×10^{-8}	4.0185×10^{-2}	5.38×10^{5}
Decagonal	9.16×10^{-5}	5×10^{-2}	546
Elliptical	6.828×10^{-3}	5.244×10^{-2}	8

TABLE II: Comparison of birefringence of different reported photonic crystal fiber and that of proposed ones

Structures	Characteristics	Birefringence	Comparison
Hexagonal	Reported [27]	1.168×10^{-2}	23 times
	Proposed	2.67×10^{-1}	higher
Octagonal	Reported [28]	2.04×10^{-2}	2 times
	Proposed	4.0185×10^{-2}	higher
Decagonal	Reported [29]	1.02×10^{-2}	5 times
	Proposed	5×10^{-2}	higher
elliptical	Reported [30]	10^{-2}	5 times
	Proposed	5.244×10^{-2}	higher

diameter used in the proposed design is 280 nm, this structure can be easily fabricated.

Here SF57 glass is used in the core. A number of works on the fabrication of a single mode SF57 glass fiber were reported in the early 2000 [25], [26]. So it is totally feasible to fabricate the proposed SF57 infiltrated fiber.

Adding this modification in the core not only improves the birefringence of the investigated fiber but also provides a higher value than any other reported structure. A comparative study has been made in Table II with the birefringence reported in very recent structures with that of proposed ones. The table helps to conclude that a multiple times higher birefringence can be ensured with this modification than the current reported configurations. Not only this, the configuration required to obtain such high value is comparatively much simpler than those of reported structures in [27], [28], [29], [30].

All the values in the table are considered at operating wavelength of 1550 nm.

IV. Conclusion

The effect of elliptical glass rod in the core region of a photonic crystal fiber on birefringence has been demonstrated. Four basic structures have been investigated by adding this modification which increases the birefringence of the fiber considerably. This investigation led to the conclusion that the birefringence of any fiber can be improved for any polarization maintaining application. This insertion enhances the polarization property of the fiber by creating a greater difference between the two fundamental modes thus birefringence is increased notably. The birefringence can be improved upto the order of 10^{-1}.

References

[1] F. Poletti, N. Wheeler, M. Petrovich, N. Baddela, E. N. Fokoua, J. Hayes, et al., "Towards high-capacity fibre-optic communications at the speed of light in vacuum," Nature Photonics, vol. 7, pp. 279-284, 2013.

[2] D. Chen and L. Shen, "Ultrahigh birefringent photonic crystal fiber with ultralow confinement loss," IEEE Photonics Technology Letters, vol. 19, pp. 185-187, 2007.

[3] W. H. Reeves, J. Knight, P. S. J. Russell, and P. Roberts, "Demonstration of ultra-flattened dispersion in photonic crystal fibers," Optics express, vol. 10, pp. 609-613, 2002.

[4] T. Monro, K. Kiang, J. Lee, K. Frampton, Z. Yusoff, R. Moore, et al., "High nonlinearity extruded single-mode holey optical fibers," in Optical Fiber Communication Conference and Exhibit, 2002. OFC 2002, 2002, pp. FA1-FA1.

[5] K. Tajima, J. Zhou, K. Nakajima, and K. Sato, "Ultralow loss and long length photonic crystal fiber," Journal of Lightwave Technology, vol. 22, p. 7, 2004.

[6] M. D. Nielsen, N. A. Mortensen, J. R. Folkenberg, A. Petersson, and A. Bjarklev, "Improved all-silica endlessly single-mode photonic crystal fiber," in Optical Fiber Communication Conference, 2003, p. FI7.

[7] J. Broeng, D. Mogilevstev, S. E. Barkou, and A. Bjarklev, "Photonic crystal fibers: A new class of optical waveguides," Optical fiber technology, vol. 5, pp. 305-330, 1999.

[8] K. Suzuki, H. Kubota, S. Kawanishi, M. Tanaka, and M. Fujita, "High-speed bi-directional polarisation division multiplexed optical transmission in ultra low-loss (1.3 dB/km) polarisation-maintaining photonic crystal fibre," Electronics letters, vol. 37, pp. 1399-1401, 2001.

[9] S. Chung, J. Kim, B.-A. Yu, and B. Lee, "A fiber Bragg grating sensor demodulation technique using a polarization maintaining fiber loop mirror," IEEE Photonics Technology Letters, vol. 13, pp. 1343-1345, 2001.

[10] D.-H. Kim and J. U. Kang, "Sagnac loop interferometer based on polarization maintaining photonic crystal fiber with reduced temperature sensitivity," Optics Express, vol. 12, pp. 4490-4495, 2004.

[11] D. S. Bethune and W. P. Risk, "An autocompensating fiber-optic quantum cryptography system based on polarization splitting of light," IEEE Journal of Quantum Electronics, vol. 36, pp. 340-347, 2000.

[12] M. Nakazawa, E. Yoshida, and Y. Kimura, "Ultrastable harmonically and regeneratively modelocked polarisation-maintaining erbium fibre ring laser," Electronics Letters, vol. 30, pp. 1603-1605, 1994.

[13] Y. Sasaki, K. Okamoto, T. Hosaka, and N. Shibata, "Polarization-maintaining and absorption-reducing fibers," in Optical Fiber Communication Conference, 1982, p. ThCC6.

[14] M. Varnham, D. Payne, R. Birch, and E. Tarbox, "Single-polarisation operation of highly birefringent bow-tie optical fibres," Electronics letters, vol. 19, pp. 246-247, 1983.

[15] J. Simpson, R. Stolen, F. Sears, W. Pleibel, J. MacChesney, and R. Howard, "A single-polarization fiber," Journal of Lightwave Technology, vol. 1, pp. 370-374, 1983.

[16] K. Tajima and Y. Sasaki, "Transmission loss of a 125-mu m diameter PANDA fiber with circular stress-applying parts," Journal of Lightwave Technology, vol. 7, pp. 674-679, 1989.

[17] A. R. Chraplyvy, "Limitations on lightwave communications imposed by optical-fiber nonlinearities," Journal of Lightwave Technology, vol. 8, pp. 1548-1557, 1990.

[18] A. Ortigosa-Blanch, J. Knight, W. Wadsworth, J. Arriaga, B. Mangan, T. Birks, et al., "Highly birefringent photonic crystal fibers," Optics letters, vol. 25, pp. 1325-1327, 2000.

[19] K. Saitoh and M. Koshiba, "Single-polarization single-mode photonic crystal fibers," IEEE Photonics Technology Letters, vol. 15, pp. 1384-1386, 2003.

[20] C.-N. Liu, T.-H. Wang, T.-S. Rou, N.-K. Chen, S.-L. Huang, and W.-H. Cheng, "Higher Gain of Single-Mode Cr-Doped Fibers Employing Optimized Molten-Zone Growth," Journal of Lightwave Technology, 2017.

[21] M. Loncar, T. Doll, J. Vuckovic, and A. Scherer,"Design and fabrication of silicon photonic crystal optical waveguides," Journal of lightwave technology, vol. 18, pp. 1402-1411, 2000.

[22] H. Kubota, S. Kawanishi, S. Koyanagi, M. Tanaka, and S. Yamaguchi, "Absolutely single polarization photonic crystal fiber," IEEE Photonics Technology Letters, vol. 16, pp. 182-184, 2004.

[23] K. Suzuki, H. Kubota, S. Kawanishi, M. Tanaka, and M. Fujita, "Optical properties of a low-loss polarization-maintaining photonic crystal fiber," Optics Express, vol. 9, pp. 676-680, 2001.

[24] D. Tee, M. A. Bakar, N. Tamchek, and F. M. Adikan, "Photonic Crystal Fiber in Photonic Crystal Fiber for Residual Dispersion Compensation Over $\mathrm{E}+\mathrm{S}+\mathrm{C}+\mathrm{L}+\mathrm{U}$ Wavelength Bands," IEEE Photonics Journal, vol. 5, pp. 7200607-7200607, 2013.

[25] T. Monro, K. Kiang, J. Lee, K. Frampton, Z. Yusoff, R. Moore, et al., "High nonlinearity extruded single-mode holey optical fibers," in Optical Fiber Communication Conference and Exhibit, 2002. OFC 2002, 2002, pp. FA1-FA1.

[26] K. Kiang, K. Frampton, T. Monro, R. Moore, J. Tucknott, D. Hewak, et al., "Extruded singlemode non-silica glass holey optical fibres," Electronics Letters, vol. 38, pp. 546-547, 2002.

[27] M. Hasan, M. Anower, M. Rashid, and S. Ali, "A polarization maintaining hexagonal photonic crystal fiber for residual dispersion compensation," in Electrical Engineering and Information Communication Technology (ICEEICT), 2016 3rd International Conference on, 2016, pp. 1-6.

[28] M. M. Rashid, M. S. Anower, M. I. Hasan, and M. R. Hasan, "Highly birefringent octagonal shaped photonic crystal fiber with two zero dispersion wavelengths in Ti: Sapphire oscillator range," in Electrical Engineering and Information Communication Technology (ICEEICT), 2016 3rd International Conference on, 2016, pp. 1-6.

[29] M. De, R. K. Gangwar, and V. K. Singh, "Designing of highly birefringence, dispersion shifted decagonal photonic crystal fiber with low confinement loss," Photonics and Nanostructures-Fundamentals and Applications, vol. 26, pp. 15-23, 2017.

[30] A. K. Ghunawat, R. Chandra, and G. Singh, "Design of an ultra-flattened negative dispersion elliptical spiral photonic crystal fiber with high nonlinearity and high birefringence," in Computer, Communications and Electronics (Comptelix), 2017 International Conference on, 2017, pp. 623-627.